Ultrasonics - Sonochemistry 63 (2020) 104967

Contents lists available at ScienceDirect

Ultrasonics - Sonochemistry

journal homepage: www.elsevier.com/locate/ultson

Synthesis of bio-functional nanoparticles from sono-responsive amino acids using high frequency ultrasound

Sukhvir Kaur Bhangu[a], Muthupandian Ashokkumar[a,*], Francesca Cavalieri[b,c,*]

[a] School of Chemistry, University of Melbourne, VIC 3010, Australia
[b] School of Science, RMIT University, Melbourne, VIC 3001, Australia
[c] Dipartimento di Scienze e Tecnologie Chimiche, Universita' degli Studi di Roma "Tor Vergata", via della ricerca scientifica 1, 00133 Rome, Italy

ARTICLE INFO

Keywords:
Ultrasound
Phenylalanine
Tryptophan
Nanoparticles
Self-assembly

ABSTRACT

A simple, one-pot high frequency ultrasonication (490 kHz) methodology to convert hydrophobic and amphipathic amino acids into nanostructures was investigated. The approach involved the oxidative coupling of aromatic amino acids (phenylalanine and tryptophan) in aqueous solutions to form high molecular weight dimers and oligomers. The role of cavitation bubble surface and ultrasonic power to trigger the out-of-equilibrium self-assembly of dimers and trimers to spherical and uniform nanostructures with controlled size has been discussed. The synthesized particles exhibited fluorescence in blue, green and red spectral regions and a strong antioxidant activity.

1. Introduction

Ultrasonically generated physical and chemical effects have been utilized to synthesize a variety of nanostructures including metal nanoparticles and protein/polymer based micro-nanobubbles and capsules [1–3]. These studies, in addition to the formation of nanoplatforms, also demonstrated that the size of the materials obtained can be controlled using various ultrasonic parameters. Moreover, recent findings of our group have demonstrated the role of cavitation bubble surface on the transformation of phenolic molecules to obtain microparticles and nanostructures [4,5]. It was manifested that the oscillating cavitation bubble surface can act as a catalytic binding site for the oxidative coupling reactions among phenol-type molecules which can later self-assemble to form micro-nanoparticles without employing any metal catalysts or enzymes [4,6]. Similarly, in our very recent work with tryptophan, experimental and computational approaches were used to unveil the role of acoustic cavitation in the formation of supramolecular nanoaggregates by dissipative self-assembly [7]. It was demonstrated that ultrasound converts tryptophan to hydroxytryptophan as well as hydroxylated tryptophan dimers and in addition, triggers (collapse of cavitation bubble) the out of equilibrium dissipative self-assembly of tryptophan dimers into nanostructures below the critical aggregation concentration.

Owing to such unique reactive surface process, high frequency ultrasound can offer straightforward synthetic route for the generation of different amino acid - based nanostructures which are of substantial interest due to their biodegradability, biocompatibility and applications in drug delivery, drug targeting, optical sensing and bioimaging and food processing [7–9]. Fan et al. [9] have exploited different dipeptide systems to obtain nanostructures. They obtained peptide-based nanoparticles formed from tryptophan-phenylalanine linkages through Zn (II) coordination. The products formed through such linkages can shift the intrinsic fluorescence of the peptide from ultraviolet to visible region. It was also reported that diphenylalanine can self-assemble by aromatic stacking interactions to form nanotubes which bear high rigidity and chemical stability [10]. Besides these reports based on self-assembly of dipeptides, very limited research has been carried out on the synthesis of nanostructures from single amino acids or mixture of amino acids.

The role of OH radicals on the oxidation and dimerization of amino acids was demonstrated using Fenton reaction, pulse radiolysis and γ-radiolysis [11–13]. It was shown that with Fenton reaction and γ-radiolysis of phenylalanine; o, m, & p-hydroxyphenylalanine together with some 2,4-dihydroxyphenylalanine, 2,3 dihydroxyphenylalanine were obtained [12]. Correspondingly, tryptophan's Fenton reaction and γ- radiolysis also led to the formation of different hydroxytryptophans, N-formylkynurenine, tryptophan dimers [14]. However, formation of nanoparticles was not reported during such reactions.

Hence, here we investigate the versatility of the hot cavitation bubble surface and radicals generated by ultrasound for the oxidative

* Corresponding authors at: School of Science, RMIT University, Melbourne, VIC 3001, Australia (F. Cavalieri).
E-mail addresses: masho@unimelb.edu.au (M. Ashokkumar), francesca.cavalieri@rmit.edu.au (F. Cavalieri).

https://doi.org/10.1016/j.ultsonch.2020.104967
Received 13 October 2019; Received in revised form 3 January 2020; Accepted 9 January 2020
Available online 10 January 2020
1350-4177/

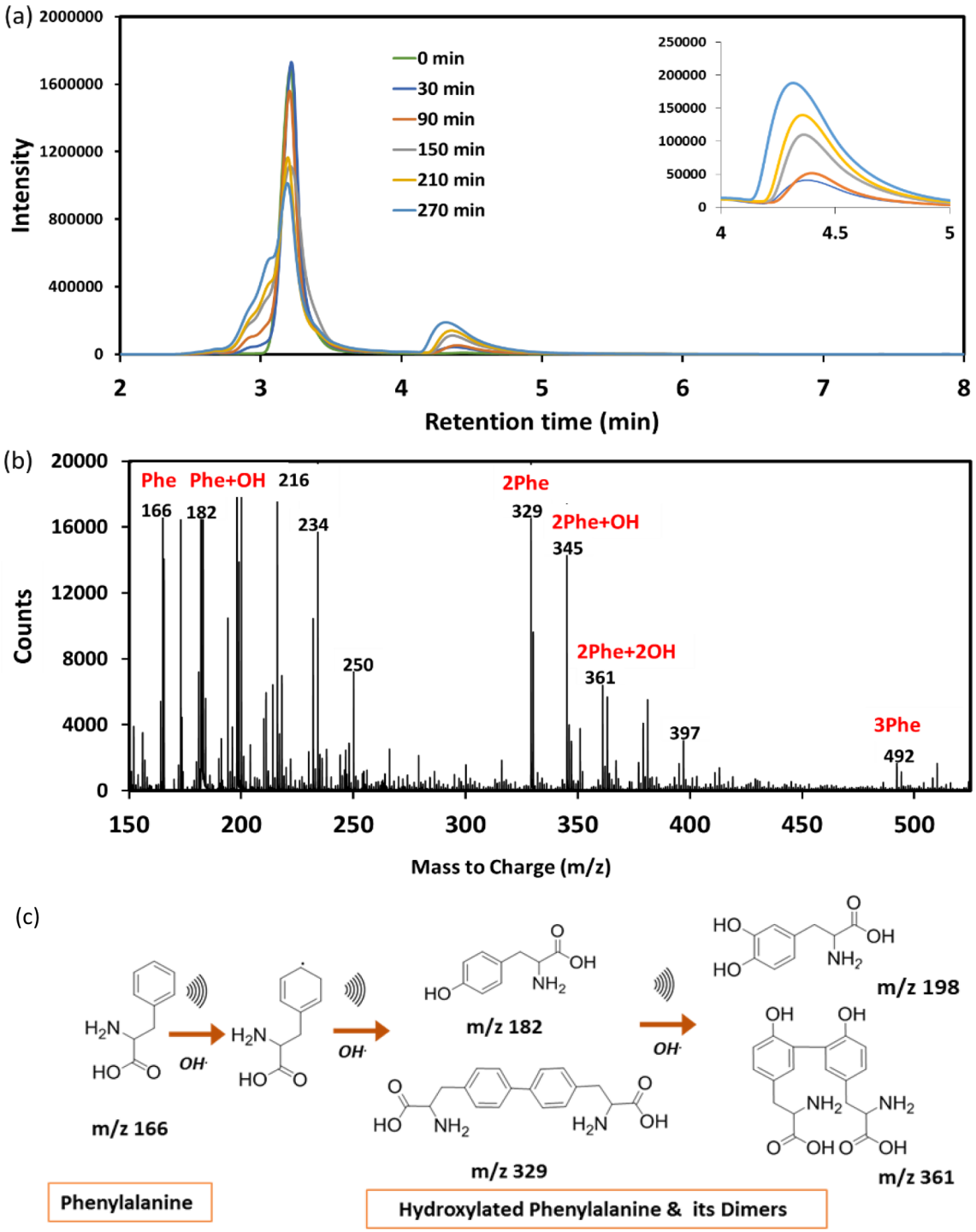

Fig. 1. (a) HPLC chromatograms of sonicated phenylalanine at 490 kHz and 4 W/cm^2 as a function of sonication time, (b) The mass spectrum of the sonicated phenylalanine at 490 kHz and 4 W/cm^2 after 5 h. and (c) A schematic of proposed mechanism for the ultrasonic driven hydroxylation and dimerization of the phenylalanine.

coupling of the phenylalanine and tryptophan when present alone or in mixture as well as for their out of equilibrium self-assembly to form supramolecular nanostructures below the critical aggregation concentration. Furthermore, ultrasonic parameters were varied to tune the size of the supramolecular nanoaggregates through controlled self-assembly. This unique methodology purveys a simple and green methodology to synthesize nanostructures from different biomolecules without the use any toxic external agents. The synthesized nanoparticles can act as a single platform for multi-disperse biological applications such as drug delivery and cellular imaging. The nanoparticles show excellent radical scavenging activity, therefore can find potential applications in biomedical fields and food processing.

2. Materials and methods

2.1. Materials

L-Tryptophan, L-phenylalanine and 1-diphenyl-2-picrylhydrazyl (DPPH) were purchased from Sigma Aldrich. HPLC grade methanol (99.9%) and formic acid were purchased from Fisher chemicals. All

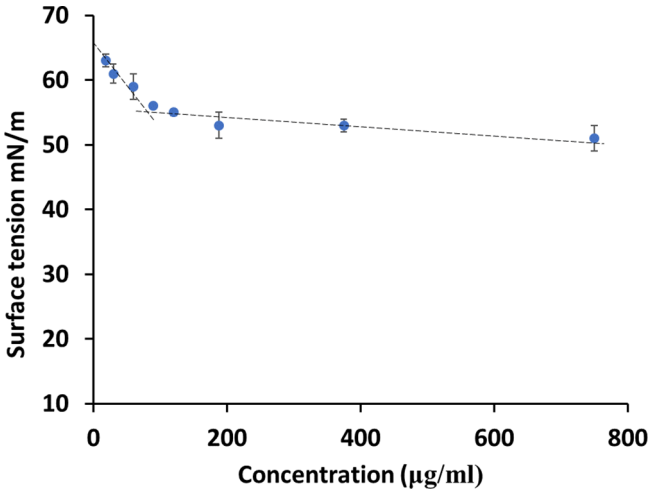

Fig. 2. Surface tension of dissolved nanoparticles obtained from phenylalanine sonication as a function of concentration.

solutions were prepared with high purity water extracted from a Millipore system with resistivity of 18.2 MΩ/cm.

2.2. Experimental details

1 mg/mL solution of phenylalanine or a 1:1 mixture containing 1 mg/mL phenylalanine and 1 mg/mL tryptophan were irradiated at an ultrasonic frequency of 490 kHz and at different ultrasonic powers of 2 W/cm^2, 4 W/cm^2 and 6 W/cm^2. The details of the methodology was reported in our previous studies [4,6]. The sonication was performed for up to 5 h. The dark brown suspension obtained was then centrifuged at 6000 rpm for 5 min and washed 3 times prior to further analysis.

2.3. Characterisation

Different characterization techniques such as scanning electron microscopy, HPLC, NMR, FTIR, mass spectrometry and absorption and fluorescence spectroscopies were used to analyse the sonicated phenylalanine and Phe:Trp mixture.

2.3.1. HPLC and mass spectrometry

HPLC analysis was performed using Shimadzu SCL-10AVP HPLC implemented with UV detector set at 205 nm and Phenomenex "Jupiter 5u C18 300A" column. The flow rate was 1 mL/min and a mixture of methanol:water:formic acid (70:30:0.5) was used as an eluent. The injection volume used was 20 µL.

Agilent Accurate-Mass QToF LC/MS in positive ion mode was used to carry out the Electrospray ionisation mass spectrometry to estimate molecular weight of the sonicated product.

2.3.2. NMR and FTIR

^{1}H NMR spectra of phenylalanine particles was conducted in d_6-DMSO on Varian MR400 NMR spectrometer at 400 MHz at 25 °C. FTIR analysis on phenylalanine and phenylalanine nanoparticles was performed on Bruker TENSOR II ATR- FTIR spectrometer. The spectra were acquired from 4000 to 400 cm^{-1} with 128 scans and 4 cm^{-1} resolution.

2.3.3. Scanning electron microscopy (SEM)

The morphology of the nanoparticles was studied by field emission scanning electron microscope (Quanta 200 FEI) at 10 kV. For Imaging analysis, a drop of nanoparticle suspension was deposited on to a metallic support with carbon tape on it and sputter coated with gold after drying.

2.3.4. Fluorescence microscopy

Fluorescence microscopy images of phenylalanine-based particles were acquired using an inverted Olympus IX71wide field microscope with 60x oil immersion objective equipped with a CCD camera (Cool SNAP FX, Photometrics, Tucson, AZ). The specimen was irradiated with illumination source under different wavelengths.

2.3.5. Fluorescence spectroscopy

The optical properties of the sonicated products were determined using Shimadzu RF-5301PC fluorescence spectrophotometer (Shimadzu) equipped with a xenon lamp and 1.0 cm optical length quartz cell. The emission and absorption spectra of the sonicated products at different sonication times were recorded in different wavelength ranges. The sonicated products were diluted in PBS pH = 7.4 prior recording the spectra.

2.3.6. Dynamic light scattering (DLS), ζ-potential

ZEN0040, Malvern Instruments was utilized to determine the zeta potential and hydrodynamic diameter of the nanoparticles. The measurement angle was 173^0 and the diameter of the particles was determined using cumulant fit method. The 80 µL nanoparticle suspension (2 mg/mL) were diluted in Milli-Q and zeta potential and hydrodynamic diameter of particles were determined

2.3.7. Surface tension measurements

The phenylalanine particles were dissolved at different concentration and surface tension was measured using pendant drop method on OCA 15 EC in water/air system.

2.3.8. Antioxidant activity

DPPH assay was conducted to measure the antioxidant activity of the phenylalanine and other sonicated mixtures. 250 µM DPPH solution was prepared in ethanol: water (50:50) mixture. Then, 100 µL solutions of 1 mg/mL phenylalanine and its mixture with tryptophan with and without sonication were added to 3 mL DPPH solution. The percentage radical scavenging activity was measured using absorption at 520 nm and the following equation:

$$\%\ Radical\ scavenging\ activity = [(A_{DPPH} - A_{sample})/A_{DPPH}] \times 100$$

where A_{DPPH} and A_{sample} are the absorption values at 520 nm for blank DPPH solution and after the addition of sample, respectively.

2.3.9. Statistical analysis

For antioxidant activity, statistical results in triplicate were analysed with Minitab 18 (Minitab LCC, Pennsylvania, USA), using one-way ANOVA with 95% confidence interval and Tukey's pairwise comparison.

3. Results and discussions

An aqueous solution of phenylalanine (1 mg/mL) was sonicated for 5 h at 490 kHz ultrasonic frequency and at different ultrasonic power levels of 2 W/cm^2, 4 W/cm^2 and 6 W/cm^2. During sonication, the color of the mixture changed from colorless to dark brown along with the formation of nanostructured products.

The composition of the nanoparticles and mechanism involved in the phenylalainine derived nanoformulation were investigated. Fig. 1a shows the HPLC chromatograms of sonicated phenylalanine solutions at different sonication times at 4 W/cm^2. A decrease in the peak area at retention time 3.5 min (corresponding to phenylalanine) along with the appearance of new peaks at early retention times are observed in Fig. 1a, which can be attributed to the (hydrophilic) hydroxylated phenylalanine species. It can also be noticed that the peak at retention time 4.4 min increases with an increase in sonication time. This peak can be attributed to the high molecular weight species formed by sonication which could be more hydrophobic since they were eluted after

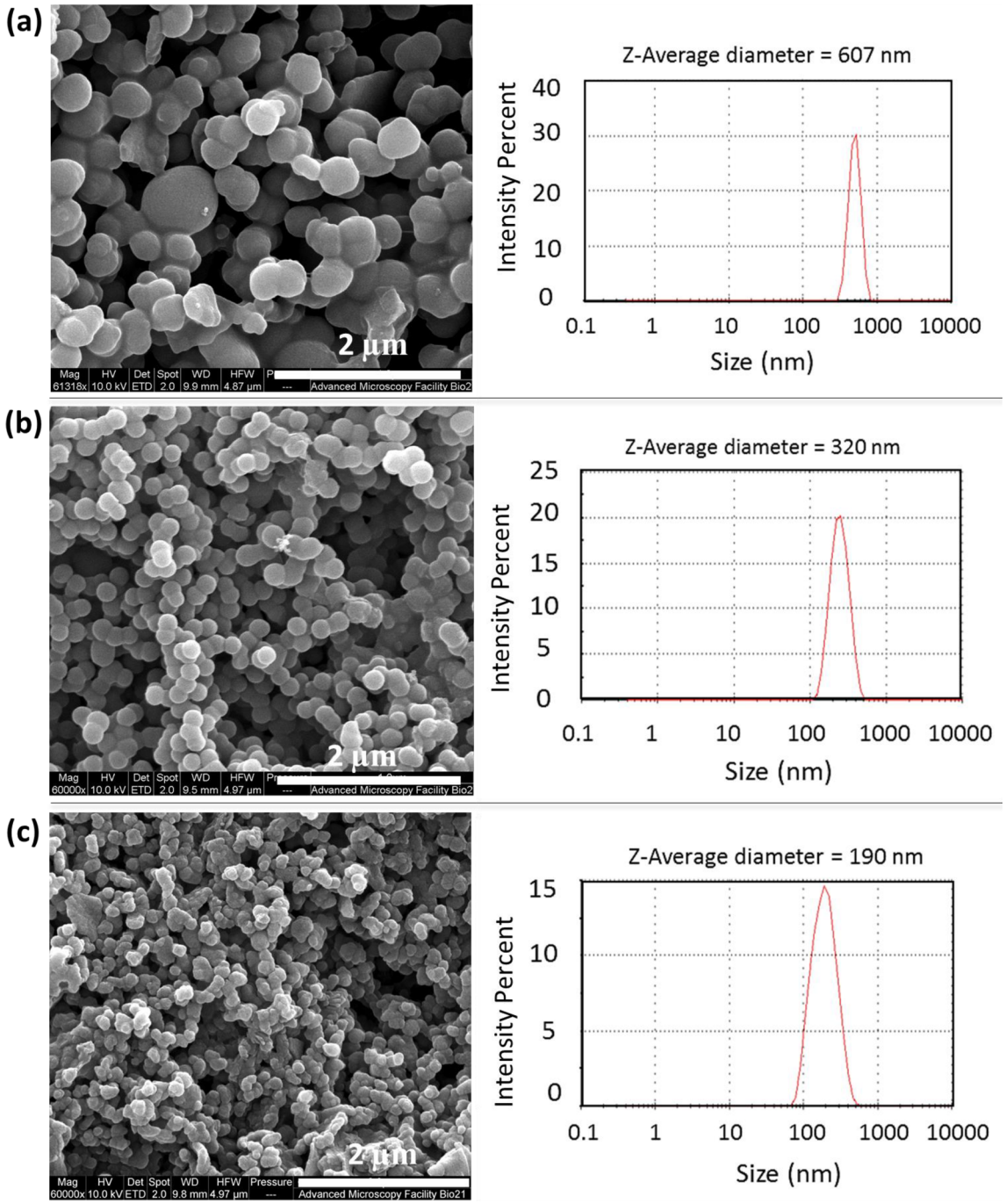

Fig. 3. SEM images and size distribution of nanoparticles obtained by sonication of phenylalanine at 490 kHz at ultrasonic powers (a): 2 W/cm^2, (b) 4 W/cm^2 and (c) 6 W/cm^2.

phenylalanine. The HPLC results are also supported by mass spectrometry analysis which confirmed the formation of dimers and trimers of phenylalanine. Fig. 1b shows the mass spectrum of sonicated phenylalanine suggesting the formation of hydroxylated phenylalanine at *m/z* 182 (Phe + OH), 198 (Phe + 2OH), dimer of phenylalanine at *m/z* 329 (Phe-Phe), hydroxylated dimers at *m/z* 345(2Phe + OH), 361 (2Phe + 2OH) and trimer of phenylalanine at *m/z* 492 (3Phe). The NMR spectra of phenylalanine nanoparticles after dissolution in DMSO is shown in Fig. S1. The peaks observed between 7.0 and 7.3 ppm were assigned to different aromatic protons in phenylalanine dimer and trimer formed through C–C linkage. The presence of different hydroxyl groups was also confirmed by peaks at 8.1 and 10.2 ppm. Additionally, FTIR analysis of phenylalanine nanoparticles also suggested the presence of OH groups as identified from the peak at 3350 cm^{-1} corresponding to OH stretch which was absent in L-phenylalanine (Fig. S2).

Fig. 1c shows the proposed mechanism along with possible structures of species obtained after the sonication of phenylalanine with respect to their mass to charge ratio. In brief, both OH radicals and adsorption of biomolecules on to the cavitation bubble surface are pivotal for the reaction to occur. The active cavitation bubbles within the ultrasonic frequency range of 200–1000 kHz have a life time of about 0.3–1 ms [15]. This could provide sufficient time for the hydrophobic amino acid molecules, depending upon their diffusion kinetics, to diffuse, adsorb and react at the bubble-solution interface. In accordance with previous studies [17,18], OH radicals generated by ultrasound can

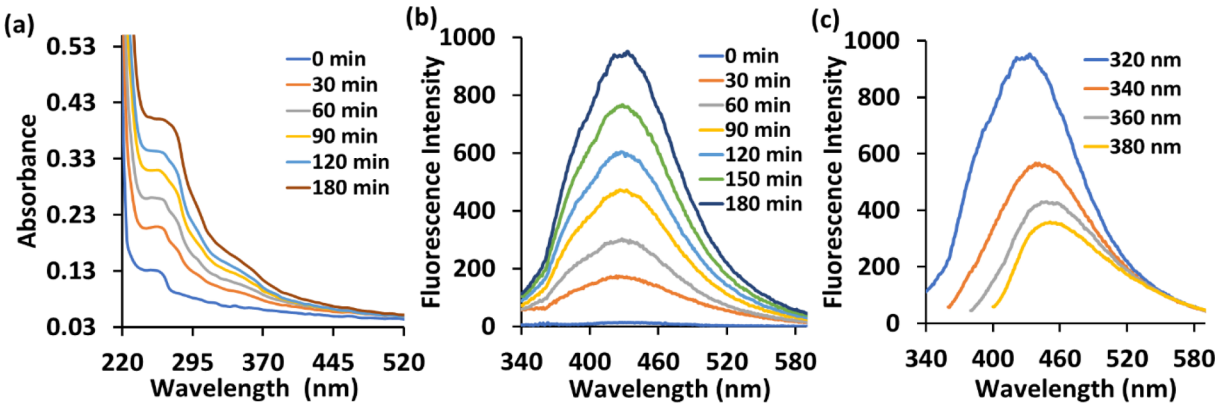

Fig. 4. (a) The absorption spectra and (b) The fluorescence emission spectra at λ_{ex} = 320 nm of the sonicated phenylalanine at different sonication times, (c) The fluorescence emission spectra of sonicated phenylalanine after 180 min at different excitation wavelengths.

abstract a proton from the aromatic ring of phenylalanine adsorbed at solution- bubble interface leading to the formation of phenyl radicals (Fig. 1c). Furthermore, the reaction between OH· and phenyl radicals could result in the formation of hydroxylated phenylalanine or two phenyl radicals can combine to form dimer of phenylalanine. Continuation of these reactions results in the formation of higher molecular weight species, which can self-assemble through different molecular interactions (H-bonding, π-π stacking) to form nanoparticles (Fig. 3b).

It was also found that phenylalanine itself at the 1 mg/mL concentration had surface tension of 70 mN/m however, surface tension of the phenylalanine dimers/trimers was 57 mM/m at concentration of 200 μg/mL (Fig. 2). This indicates that the dimers/trimers are more surface active and can undergo self-assembly at much lower concentration.

The cac (critical aggregation concentration) of nanoparticles, which are composed of hydroxylated dimer and trimer of phenylalanine, was determined from surface tension measurements after dissolution was ~80 μg/mL (Fig. 2). However, the concentration at which aggregates were formed during sonication was ~50 μg/mL. The nanoparticles rapidly dissolved at this concentration when pH was increased to 11 and were unable to re-assemble after the pH was brought back to acidic. On the other hand, when ultrasound was applied to this solution of nanoparticles in acidic environment, it successfully led to the formation of nanoaggregates. Therefore, in accordance to previous findings [7] the self-assembly of phenylalanine-based nanoparticles was also found to be out of equilibrium and was taking place below cac where ultrasound besides the formation of dimer and trimer of phenylalanine can trigger the formation of nanoaggregate through dissipative self-assembly.

It is also worth mentioning that enhanced conjugation of phenylalanine (through formation of dimers and trimers) would increase its hydrophobicity (as seen from HPLC and surface tension measurements) that would lead to increase of π-π interactions required for the self-assembly. Moreover, the presence of multiple OH groups is likely also important to assist the self-assembly through H-bonding. Hence, both π-π interactions and H-bonding play crucial role in the self-assembly of phenylalanine dimers and trimers to form nanoparticles.

The effect of ultrasonic power on the size of phenylalanine nanoparticles was investigated. Fig. 3a, b and c show SEM images of the particles obtained by sonication of phenylalanine at different acoustic power levels- 2 W/cm^2, 4 W/cm^2 and 6 W/cm^2, respectively. It can be observed that the particles have spherical morphology and their size decrease with an increase in power. The hydrodynamic radius of the particles and particle size distribution were determined by dynamic light scattering. The Z-average size of the particles decreased from 607 ± 88 nm to 190 ± 50 nm when the power density was switched from 2 to 6 W/cm^3 (Fig. 3a–c). The effect of ultrasonic power on the size has been demonstrated several times [16]. With increasing power, the acoustic cavitation activity is known to be enhanced. There occurs two types of cavitation bubbles; stable (oscillate for hundreds of acoustic cycles) and transient bubbles (live for few acoustic cycles) [17,18]. A higher amplitude (higher power) would increase the number of transient and active bubbles. More transient energy input due to the collapse of acoustic bubble would increase the rate of nucleation. A higher nucleation rate would lead to a reduction in the size of nanoparticles as the rate of nucleation and radius are inversely related to each other [19,20]. Based on this hypothesis, a reduction in nanoparticle size could be expected at high power levels. The zeta potential of the nanoparticles was around −30 ± 6 mV providing colloidal stability to the particles. The particles were negatively charged due to the deprotonation of the carboxyl and aromatic hydroxyl groups in water at pH 7.

The self -assembly of dimers and trimers to form nanostructures is further discussed based on absorption, fluorescence and solubility studies of the nanoparticles. Fig. 4a shows the absorption spectra of sonicated phenylalanine at different sonication times. Absorption spectra show new bands around 310 nm and 350 nm with increase in sonication time together with an overall increase in absorption. The trend observed is similar to that observed during the polymerization of aromatic phenolic molecules, where enhanced conjugation led to new absorption bands at higher wavelengths with an increase in absorption suggesting an increase in conjugation with an increase in sonication time [6,21].

Fig. 4b shows the fluorescence emission spectra of sonicated phenylalanine at different sonication times at an excitation wavelength of 320 nm. A new emission band centered at 430 nm can be observed which was increasing with the time of sonication. It is known that the monomeric form of phenylalanine does not exhibit any fluorescence in the wavelength range of 400–600 nm, thus this new emission could be due to the conjugated system i.e.; dihydroxyphenylalanine and dimers of phenylalanine [22,23]. Fig. 4c illustrates the fluorescence excitation spectra of phenylalanine after 3 h ultrasonic irradiation at different excitation wavelengths. The shift in fluorescence emission maximum from 430 nm to 460 nm was observed when excitation wavelength was changed from 320 nm to 380 nm. These results suggest the presence of multiple species which is in accordance with the mass spectrometry analysis. The red shift and broadening of absorption and fluorescence spectra also indicate π-π interactions between aromatic moieties.

Moreover, the optical properties of the phenylalanine-derived particles obtained by high frequency sonication were investigated. Fig. 5a shows the dependence of emission spectra on excitation wavelength where a shift in emission maximum from 445 nm to 530 nm can be observed with a change in excitation wavelength from 340 nm to 500 nm. This shift could be attributed to the presence of different hydroxylated, dimeric and trimeric species. On the other hand, new bands with maxima at 610 nm and 670 nm were also observed at higher excitation wavelengths of 560 and 600 nm, respectively. The respective

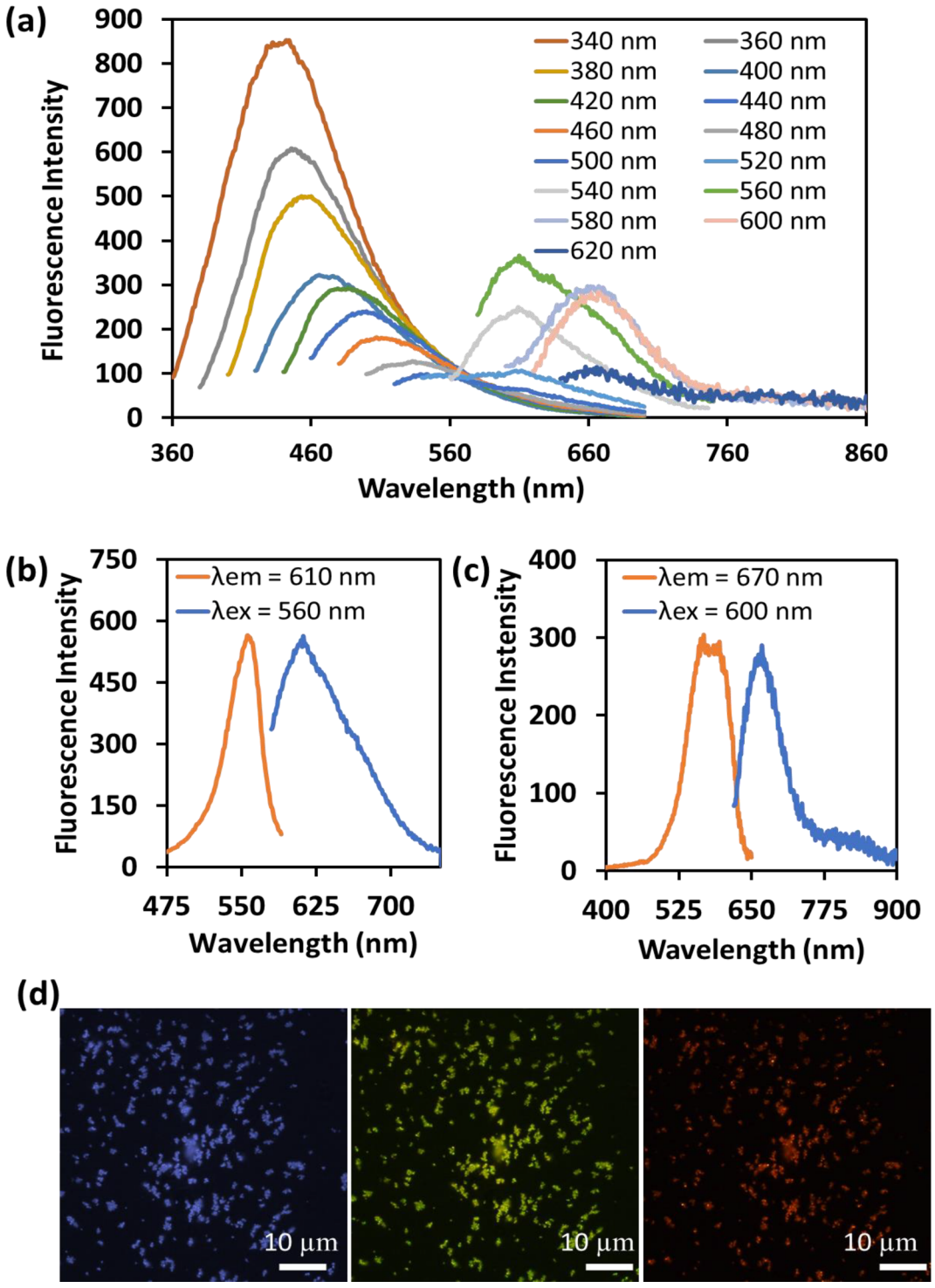

Fig. 5. (a) The dependence of fluorescence emission spectra on the excitation wavelengths from 340 nm to 600 nm of the phenylalanine nanoparticles, (b) The fluorescence emission and excitation spectra of the phenylamine nanoparticles at λ_{ex} = 560 nm and λ_{em} = 610 nm, respectively. (c) The fluorescence emission and excitation spectra of the phenylalanine nanoparticles at λ_{ex} = 600 nm and λ_{em} = 670 nm, respectively, and (d) The fluorescence microscopic images of phenylalanine nanoparticles showing the blue, green and red fluorescence. (For interpretation of the references to color in this figure legend, the reader is referred to the web version of this article.)

excitation spectra of emission spectra are provided in Fig. 5b and c. The red shift and bands at higher wavelengths might suggest electron delocalization which again indicates strong π-π interactions between the high molecular weight species obtained by sonication. The fluorescence of the nanoparticles in blue, green and red region was also confirmed by fluorescence microscopy as shown in Fig. 5d.

In addition, the mixture of phenylalanine and tryptophan at the same concentration (1 mg/mL) was sonicated using the same experimental condition to obtain nanoparticles and Fig. 6a shows the nanoparticles obtained after the sonication of Phe:Trp (1:1) mixture. These particles also exhibit spherical morphology with Z- average size of the nanoparticles about 385 nm ± 65 nm. Fig. 6b shows the fluorescence emission spectra of Phe:Trp nanoparticles at different excitation wavelengths. The emission peaks in the wavelength range of 400–480 nm

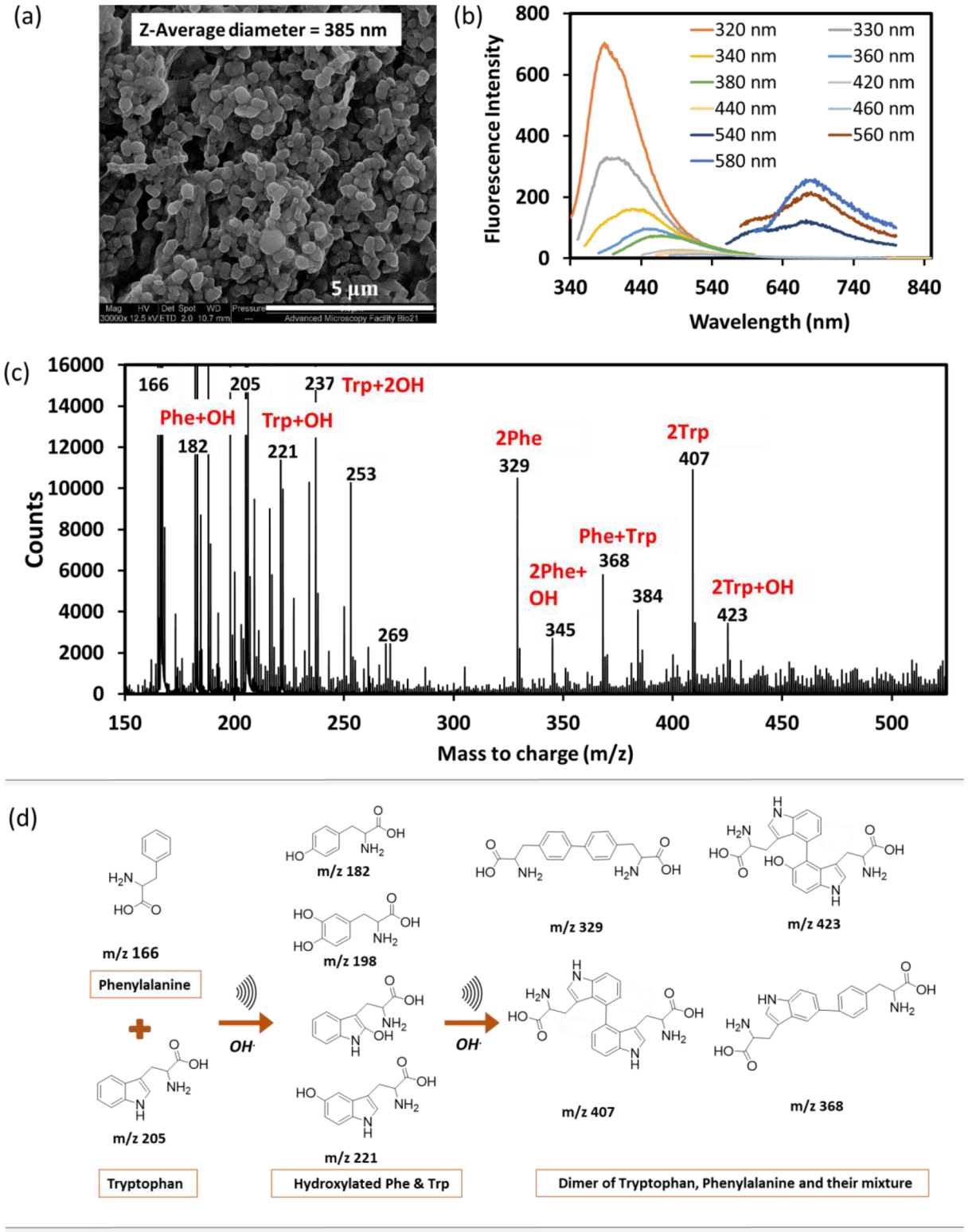

Fig. 6. Sonication of Phe:Trp (1:1) at 490 kHz and 5 W/cm^3 (a) SEM image of the nanoparticles obtained after sonication, (b) The dependence of fluorescence emission spectra on excitation wavelengths from 320 to560 nm of Phe:Trp nanoparticles, (c) Mass spectra of the sonicated mixture of Phenylalanine and tryptophan and (d) The schematic and proposed mechanism for the ultrasonic driven hydroxylation and dimerization of the phenylalanine and tryptophan.

were observed. As mentioned before, phenylalanine and tryptophan do not exhibit emission in the range of 400–480 nm. Therefore, these emissions peaks can be attributed to the increased conjugation due to the formation of high molecular weight products. Moreover, higher shift in emission and excitation wavelengths to 690 nm and 580 nm respectively yet again suggest intermolecular interaction (H bonding and π-π interactions) among different molecules to self-assemble into nanoparticles. Fig. 6b shows the mass spectrum of the mixture of tryptophan and phenylalanine. It shows the formation of hydroxylated and high molecular weight species of phenylalanine (similar to

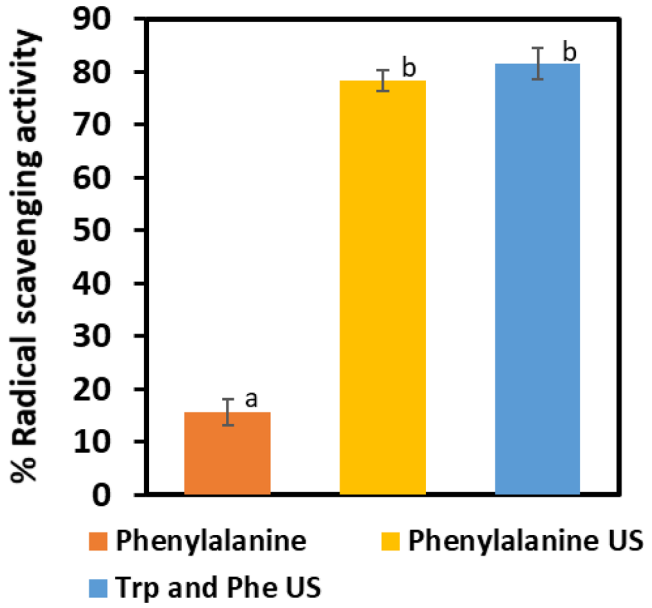

Fig. 7. The percentage DPPH radical scavenging of Phenylalanine in comparison with sonicated phenylalanine and its mixture with Tryptophan after 2 min incubation with DPPH solution and final concentration of 30 μg/mL. The significantly different values ($p < 0.05$) between the bars are denoted by alphabets.

observed in Fig. 1b during phenylalanine sonication) along with variety of other products. For instance, hydroxylated tryptophan at m/z 221, dimer of tryptophan at m/z 407 and phenylalanine and tryptophan linkage suggested by peak at m/z 368, hydroxylated tryptophan dimer at m/z 423. Fig. 6d illustrates the proposed mechanism and structures of the products formed by sonication of Trp:Phe mixture. Tryptophan bears different sites for OH radical attack. OH radicals can attack the pyrrole moiety of the tryptophan to extract a proton and to form hydroxytryptophan at different positions [6]. The Trp and Phe radicals can also react with each other to form Trp-Phe or they can combine with their own radical to form dimers and trimers.

Overall these results show a new approach to synthesize phenylalanine and tryptophan- phenylalanine based nanoparticles using merely aqueous solutions of aromatic amino acids and high frequency sonication, without the use of any external agents. These amino acid-based nanostructures owing to their fluorescent properties can be ideally used for live cell bioimaging, or as a platform for the loading of any hydrophobic drugs.

To evaluate the functional properties of the synthesized nanoparticles, the antioxidant activity of the particles was studied. It is also worth noting that phenylalanine nanoparticles can be used as such for different application without any further purification or separation step. Most antioxidant molecules bear high degree of hydroxylation. As mentioned, sonication results in the addition of OH groups and the oligomerization of biomolecules also tend to enhance the degree of hydroxylation. The DPPH radical scavenging assay was carried out to quantify the antioxidant activity. Fig. 7 shows the radical scavenging activity of phenylalanine in comparison with its sonicated analogues at the same concentration. It can be noted that the phenylalanine itself has a very limited radical scavenging activity of 10%. Conversely, sonicated phenylalanine and phenylalanine/tryptophan particles after dissolution exhibited 80% radical scavenging activity within 2 min of incubation with DPPH radical. Therefore, these results show that the ultrasonic treatment of aromatic amino acids and assembly into nanoparticles can significantly enhance the antioxidant activity of the native biomolecules. These nanoparticles apart from being fluorescent and to be used in bioimaging can potentially protect the cells against any oxidative damage due to free radicals. This activity was shown for instance for different polyphenolic nanoparticles [24]. Moreover, they can find potential applications as preservatives in food (meat, dairy, oils etc) as they can inhibit the oxidative rancidity.

The current ultrasonic approach has a versatile applicability as it can be utilized to generate nanoformulation from different types of aromatic biomolecules. Depending on the types of biomolecules and ultrasonic parameters the properties of the nanostructures can be tuned.

4. Conclusions

The study, in order to expand the knowledge base in the area of ultrasound-driven synthesis of nanoformulations, has explored the use of high frequency ultrasound as a new approach for the synthesis of nanostructures from single aromatic amino acids. The size of the nanostructures can be controlled using different ultrasonic parameters. The new strategy applied in this study illustrated the role of cavitation bubble surface and OH radicals to carry out hydroxylation, oligomerization and out of equilibrium self-assembly of phenylalanine and tryptophan to form spherical nanostructures. The nanostructures formed, together with significant antioxidant properties, have fluorescence in blue, green and red spectral region. Hence, they can be utilized as bioimaging probes for live cell imaging and can also find potential applications as food preservatives. The current ultrasonic approach can be extended to other aromatic biomolecules for the construction of different nanostructures for multifarious biological and other applications.

Declaration of Competing Interest

The authors declare that they have no known competing financial interests or personal relationships that could have appeared to influence the work reported in this paper.

Acknowledgements

This work was supported by the Australian Research Council (ARC) under a Future Fellowship (F. Cavalieri, FT140100873). We acknowledge the University of Melbourne for their support through MRS scholarship.

Appendix A. Supplementary data

Supplementary data to this article can be found online at https://doi.org/10.1016/j.ultsonch.2020.104967.

References

[1] R.A. Caruso, M. Ashokkumar, F. Grieser, Sonochemical formation of gold sols, Langmir 18 (2002) 7831–7836.
[2] Aashima, S.K. Pandey, S. Singh, S.K. Mehta, Ultrasonication assisted fabrication of l-lysine functionalized gadolinium oxide nanoparticles and its biological acceptability, Ultrason. Sonochem. 49 (2018) 53–62.
[3] F. Cavalieri, M. Colone, A. Stringaro, M. Tortora, A. Calcabrini, M. Zhou, M.J.P. Ashokkumar, P.S. Characterization, Influence of the morphology of lysozyme-shelled microparticles on the cellular association uptake, and degradation in human breast adenocarcinoma cells, Part Part. Syst. Char. 30 (2013) 695–705.
[4] F. Cavalieri, E. Colombo, E. Nicolai, N. Rosato, M. Ashokkumar, Sono-assembly of nanostructures via tyrosine–tyrosine coupling reactions at the interface of acoustic cavitation bubbles, Mater. Horiz. 3 (2016) 563–567.
[5] S.K. Bhangu, R. Singla, E. Colombo, M. Ashokkumar, F. Cavalieri, Sono-transformation of tannic acid into biofunctional ellagic acid micro/nanocrystals with distinct morphologies, Green Chem. 20 (2018) 816–821.
[6] S.K. Bhangu, G. Bocchinfuso, M. Ashokkumar, F. Cavalieri, Sound-driven dissipative self-assembly of aromatic biomolecules into functional nanoparticles, Nanoscale Horiz. (2020.).
[7] M. Ayoub, D. Scheidegger, Peptide drugs, overcoming the challenges, a growing business, Chim. Oggi 24 (2006) 46–48.
[8] P. Cheruku, J.-H. Huang, H.-J. Yen, R.S. Iyer, K.D. Rector, J.S. Martinez, H.-L. Wang, Tyrosine-derived stimuli responsive, fluorescent amino acids, Chem. Sci. 6 (2015) 1150–1158.
[9] Z. Fan, L. Sun, Y. Huang, Y. Wang, M. Zhang, Bioinspired fluorescent dipeptide

nanoparticles for targeted cancer cell imaging and real-time monitoring of drug release, Nat. Nanotech. 11 (2016) 388–394.
[10] M. Reches, E. Gazit, Molecular self-assembly of peptide nanostructures: mechanism of association and potential uses, Curr. Nanosci. 2 (2006) 105–111.
[11] J. Chrysochoos, Pulse radiolysis of phenylalanine and tyrosine, Radiat. Res. 33 (1968) 465–479.
[12] Z. Maskos, J. Rush, W. Koppenol, The hydroxylation of phenylalanine and tyrosine: a comparison with salicylate and tryptophan, Arch. Biochem. Biophys. 296 (1992) 521–529.
[13] A. Galano, A. Cruz-Torres, OH radical reactions with phenylalanine in free and peptide forms, Org. Biomol. Chem. 6 (2008) 732–738.
[14] Z. Maskos, J. Rush, W. Koppenol, The hydroxylation of tryptophan, Arch. Biochem. Biophys. 296 (1992) 514–520.
[15] L. Dharmarathne, M. Ashokkumar, F. Grieser, Reaction of ferricyanide and methyl viologen with free radicals produced by ultrasound in aqueous solutions, J. Phys. Chem. A 116 (2012) 7775–7782.
[16] D. Gao, Z. Li, Q. Han, Q. Zhai, Effect of ultrasonic power on microstructure and mechanical properties of AZ91 alloy, Mat. Sci. Eng. A 502 (2009) 2–5.
[17] M. Ashokkumar, F. Grieser, A comparison between multibubble sonoluminescence intensity and the temperature within cavitation bubbles, J. Am. Chem. Soc. 127 (2005) 5326–5327.
[18] M. Ashokkumar, M. Hodnett, B. Zeqiri, F. Grieser, G.J. Price, Acoustic emission spectra from 515 kHz cavitation in aqueous solutions containing surface-active solutes, J. Am. Chem. Soc. 129 (2007) 2250–2258.
[19] S. Kaur Bhangu, M. Ashokkumar, J. Lee, Ultrasound assisted crystallization of paracetamol: crystal size distribution and polymorph control, Cryst. Growth Des. 16 (2016) 1934–1941.
[20] J. Lee, S. Yang, Antisolvent sonocrystallisation of sodium chloride and the evaluation of the ultrasound energy using modified classical nucleation theory, Crystals 8 (2018) 320.
[21] P.K. Jha, G.P. Halada, The catalytic role of uranyl in formation of polycatechol complexes, Chem. Cent. J. 5 (2011) 12.
[22] G.J. Smith, T.G. Haskell, The fluorescent oxidation products of dihydroxyphenylalanine and its esters, J. Photochem. Photobiol. B 55 (2000) 103–108.
[23] D.A. Malencik, J.F. Sprouse, C.A. Swanson, S.R. Anderson, Dityrosine: preparation, isolation, and analysis, Anal. Biochem. 242 (1996) 202–213.
[24] F. Felice, Y. Zambito, E. Belardinelli, C. D'Onofrio, A. Fabiano, A. Balbarini, R. Di Stefano, Delivery of natural polyphenols by polymeric nanoparticles improves the resistance of endothelial progenitor cells to oxidative stress, Eur. J. Pharm. Sci. 50 (2013) (2013) 393–399.